Supporting Information

Interplay between Nanoparticle Wrapping and Clustering of Inner Anchored Membrane Proteins

TongtaoYue[*,†,‡] , Shixin Li[†,‡], Yan Xu[‡], Xianren Zhang[§], and Fang Huang[*,†,‡]

[†]State Key Laboratory of Heavy Oil Processing, [‡]Center for Bioengineering and Biotechnology, China University of Petroleum (East China), Qingdao, 266580, China.
[§]State Key Laboratory of Organic-Inorganic Composites, Beijing University of Chemical Technology, Beijing, 100029, China.

S1. Methods

Dissipative particle dynamics. The DPD method, which is a coarse-grained simulation technique with hydrodynamic interactions, was first introduced to simulate the hydrodynamic behaviors of complex fluids.[1-3] Recently, it has become one of the most commonly used computer simulation techniques to study the biomembrane system, especially on the interaction between membranes and NPs.[4-7] In DPD, the dynamics of each elementary unit is governed by Newton's equation of motion, $dr_i/dt=v_i$ and $dv_i/dt=f_i/m_i$, similar to the molecular dynamics simulation method. Typically, beads i and j interact with each other via a pairwise additive force consisting of a conservative force F_{ij}^C, a dissipative force F_{ij}^D and a random force F_{ij}^R,

$$F_i = \sum_{i \neq j} (F_{ij}^C + F_{ij}^D + F_{ij}^R) \tag{1}$$

The conservative force, which is soft and repulsive, is determined by

$$F_{ij}^C = a_{ij} \tilde{r}_{ij} \max\{1 - r_{ij}/r_c, 0\} \tag{2}$$

where a_{ij} is the maximum repulsive force constant between beads i and j, $r_{ij} = r_j - r_i$ (r_i and r_j are their positions), $\tilde{r}_{ij} = | r_{ij} | / r_{ij}$, and r_c is the cut off radius.

The dissipative force has the form

$$F_{ij}^D = -\gamma (1 - r_{ij}/r_c)^2 (\tilde{r}_{ij} \cdot v_{ij}) \tilde{r}_{ij} \tag{3}$$

where γ is the friction coefficient, $v_{ij} = v_j - v_i$ (v_i and v_j are their velocities). This expression is chosen to conserve the momentum of each pair of beads, and thus the total momentum of the system is conserved.

The random force between beads i and j is calculated by

$$F_{ij}^R = -\sigma (1 - r_{ij}/r_c)^2 \theta_{ij} \tilde{r}_{ij} \tag{4}$$

where σ represents the noise amplitude, and θ_{ij} is an uncorrelated random variable with zero mean and unit variance.

For lipid and protein molecules, the interaction between neighboring beads within the same molecule is described by a harmonic spring force,

$$F_S = K_S(r_{ij} - r_{eq})\tilde{r}_{ij} \quad (5)$$

where K_S and r_{eq} are the spring constant and the equilibrium bond length, respectively. The numerical values of K_S and r_{eq} used for our simulations are 128 and 0.7, respectively.

In order to maintain the bending rigidity of the lipids and proteins, the force constraining the variation of the bond angle is given by

$$F_\varphi = -\nabla U_\varphi \text{ and } U_\varphi = K_\varphi(1 - \cos(\varphi - \varphi_0)) \quad (6)$$

where φ_0 is set to π and K_φ is the bond bending force constant. For the lipid molecules the value of K_φ is set to 10.0, while for proteins it is set to 100.0 to make the protein rigid.

Interaction parameters. In order to reproduce the structure and thermodynamic behavior of lipid bilayer, the interaction parameters between beads of the same type were set to a_{WW} = a_{HH} = 25 and a_{TT} = 15, and those between the different types of beads were a_{TW} = 80, a_{HT} = 50, and a_{HW} = 25. Note that in DPD simulation method, all interactions are repulsive. If an interaction parameter in our simulation system is larger than 25 (the water-water interaction), the corresponding interaction can be effectively regarded as repulsive. On the other hand, if the interaction parameter is smaller than 25, the corresponding interaction is effectively attractive. Thus, to represent the strong attraction between ligands and receptors, the interaction parameter a_{LR_H} was set to 4.0. Except the ligand-receptor interaction, interaction parameters associated with receptors (R) were set to the same as those for lipids in the membrane. In Table S1 we list all the interaction parameters used in this work.

Table S1 Interaction parameters used in our simulations

	W	H	T	R_H	R_T	P_H	P_T	NP	L
W	25	25	80	25	80	25	80	50	50
H	25	25	50	25	50	25	50	25	25
T	80	50	15	50	15	50	15	80	80
R_H	25	25	50	25	50	25	50	25	4
R_T	80	50	15	50	15	50	15	80	80
P_H	25	25	50	25	50	25	50	25	25
P_T	80	50	15	50	15	50	15	80	80
NP	50	25	80	25	80	25	80	50	50
L	50	25	80	4	80	25	80	50	50

N-varied DPD method. In this work, all simulations are performed in N-varied VT ensembles, in which the targeted membrane tension can be controlled by monitoring the lipid number per area (LNPA) in a boundary membrane region.[8] The boundary region, which surrounds the central square region of the membrane, plays a role as the lipid reservoir. By adding or deleting lipids, the value of LNPA in the boundary region is kept within a defined range ($\rho_{LNPA}^{\min} < \rho_{LNPA} < \rho_{LNPA}^{\max}$). In an addition move, a number of lipid molecules are inserted into the boundary region if the local lipid area density is less than $\rho_{LNPA}^{\min}$. Conversely, if the average area density of lipids in the boundary region exceeds $\rho_{LNPA}^{\max}$, a corresponding number of lipids are deleted randomly from the boundary region. In order to keep the whole density of the beads in the simulation box constant, a corresponding number of water beads are randomly added or deleted simultaneously. In practice, the addition or deletion move was performed every 1000 time steps in order to leave enough time to propagate the tension to the whole membrane.

Free energy calculations. To energetically understand the preferential location of IAMPs in membrane with NP wrapping, we calculated the free energy change that transfers one IAMP from distant region to the bottom region of NP wrapping. To generate different initial configurations, we artificially insert the IAMP in membrane with defined distance between IAMP and NP center. Here, the thermodynamic integration approach was applied to analyze the free energy change as a function of the distance $d(\gamma)$, where $\gamma = 0$ when the IAMP locates beneath the NP wrapping. [9, 10] As the IAMP moves away from NP wrapping, γ increases and finally reaches 1 when the IAMP is distant from NP. The free energy change, ΔF, is expressed as:

$$\Delta F = \int_0^{\gamma} \frac{\partial F(\gamma)}{\partial \gamma} d\gamma \tag{7}$$

For each chosen value of γ, a harmonic potential is imposed to confine the motion of IAMP in the x-y plane:

$$U(\gamma) = k[D - d(\gamma)]^2 \tag{8}$$

Where k = 10 and $d(\gamma)$ are the spring constant and equilibrium distance between IAMP and NP, respectively. D is the actual distance between IAMP and NP. Under the harmonic potential, the IAMP is forced to oscillate around $\langle d \rangle$ in the vicinity of $d(\gamma)$, where $\langle d \rangle$ is the ensemble averaged distance between IAMP and NP. To ensure that the obtained profiles are well equilibrated, a 50000 time steps DPD simulation was performed for each chosen value of γ. Then the derivative of the free energy is determined from the constrained interaction as:

$$\frac{\partial F(\gamma)}{\partial \gamma} = \left\langle \frac{\partial U(\gamma)}{\partial \gamma} \right\rangle = 2k[\langle D \rangle - d(\gamma)] \quad d(\gamma = 0) \tag{9}$$

Integrating this expression allows to determine the change of free energy as a function of distance between IAMP and NP,

$$\Delta F = \int_{d(\gamma=0)}^{d(\gamma=\varepsilon)} 2k[d(\gamma) - \langle D \rangle] d\gamma \tag{10}$$

S2. Figures

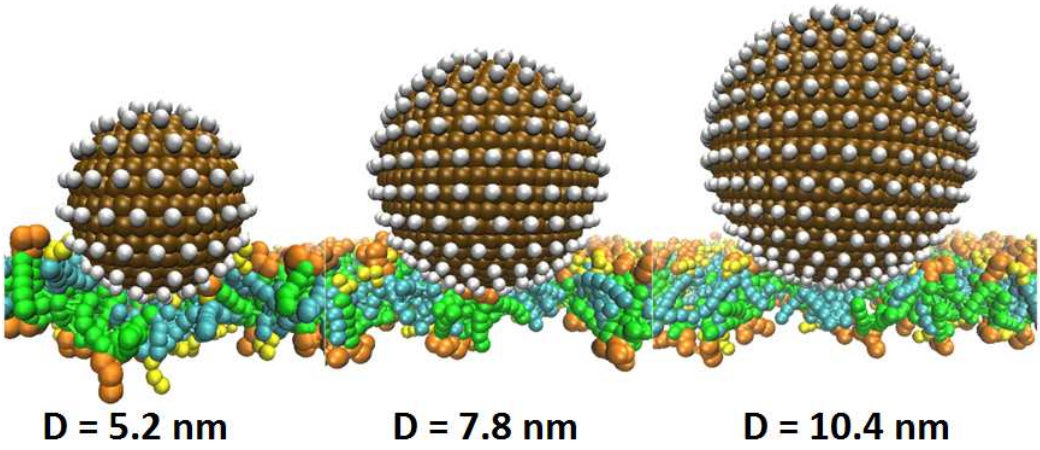

Figure S1. Local configuration of initial NP adhesion on membrane surface in the absence of IAMPs. This figure is to explain why smaller NP reaches a higher contact percentage after adhesion completes. Apparently, adjacent receptors can extend upward to contact with the ligands. Under the same extension range, smaller NPs can reach a higher ratio of ligands that contact with the receptors.

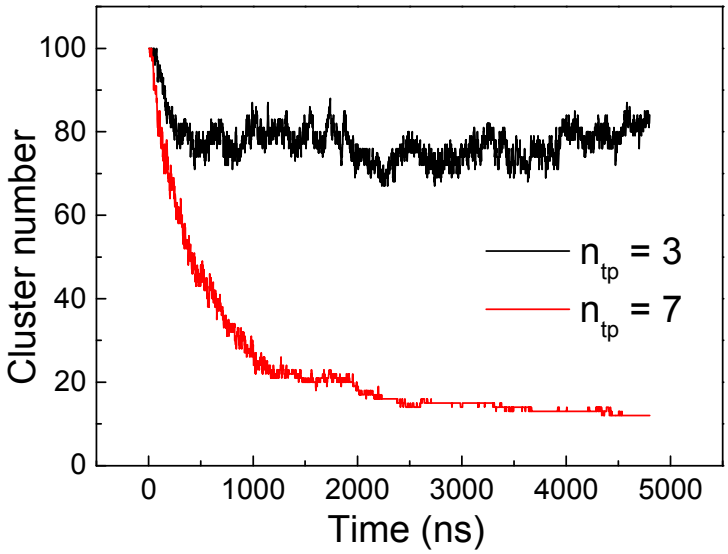

Figure S2. Time evolutions of cluster number of IAMPs with different hydrophobic lengths. This figure apparently suggests that both rate and extent of clustering of IAMPs are strongly dependent on the hydrophobic length.

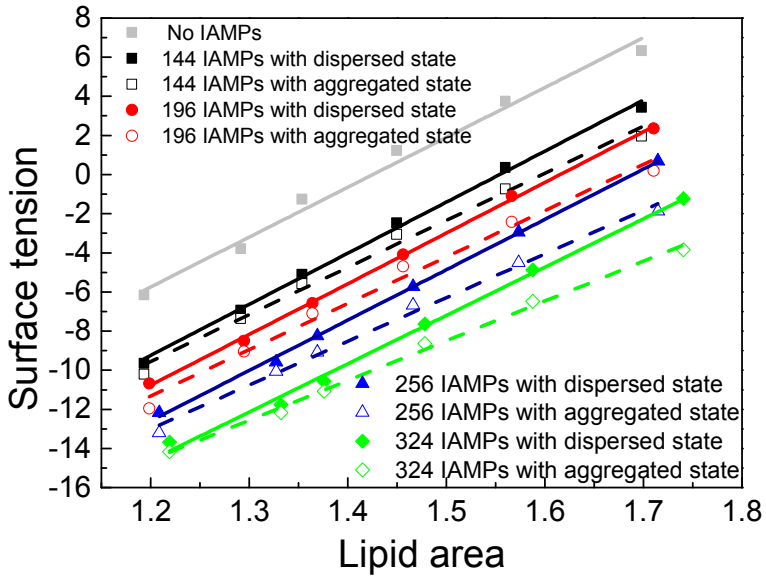

Figure S3. The calculated surface tension as a function of lipid area. For comparison, the curve for pure membrane without IAMPs was provided (gray line). In the presence of IAMPs with each density, two values of tension were calculated, corresponding to the dispersed state (solid line) and aggregated state (dashed line).

References

1. Hoogerbrugge, P. J.; Koelman, J. M. V. A. Simulating Microscopic Hydrodynamic Phenomena with Dissipative Particle Dynamics. *Europhys. Lett.* **1992**, 19, 155.
2. Español, P.; Warren, P. Statistical Mechanics of Dissipative Particle Dynamics. *Europhys. Lett.* **1995**, 30, 191.
3. Groot, R. D.; Warren, P. B. Dissipative particle dynamics: Bridging the gap between atomistic and mesoscopic simulation. *J. Chem. Phys.* **1997**, 107, 4423.
4. Shillcock, J. C.; Lipowsky, R. Tension-induced fusion of bilayer membranes and vesicles. *Nat. Mater.* **2005**, 4, 225-228.
5. Guo, R.; Mao, J.; Yan, L. T. Unique dynamical approach of fully wrapping dendrimer-like soft nanoparticles by lipid bilayer membrane. *ACS Nano* **2013**, 7, 10646-10653.
6. Alexeev, A.; Uspal, W. E.; Balazs, A. C. Harnessing janus nanoparticles to create controllable pores in membranes. *ACS Nano* **2008**, 2, 1117-1122.
7. Arai, N.; Yasuoka, K.; Zeng, X. C. A vesicle cell under collision with a Janus or homogeneous nanoparticle: translocation dynamics and late-stage morphology. *Nanoscale* **2013**, 5, 9089-9100.
8. Yue, T. T.; Li, S. Y.; Zhang, X. R.; Wang, W. C. The relationship between membrane curvature generation and clustering of anchored proteins: a computer simulation study. *Soft Matter* **2010**, 6, 6109-6118.
9. Li, Y.; Li, X.; Li, Z.; Gao, H. Surface-structure-regulated penetration of nanoparticles across a cell membrane. *Nanoscale* **2012**, 4, 3768-3775.
10. Yue, T.; Zhang, X.; Huang, F. Membrane monolayer protrusion mediates a new nanoparticle wrapping pathway. *Soft Matter* **2014**, 10, 2024-2034.